Published online April 24, 2009; doi:10.1130/B26473.1

500 m.y. of thermal history elucidated by multi-method detrital thermochronology of North Gondwana Cambrian sandstone (Eilat area, Israel)

Pieter Vermeesch[1†], Dov Avigad[2], and Michael O. McWilliams[3]
[1]*School of Earth Sciences, Birkbeck, University of London, Malet Street, London, WC1E 7HX, UK*
[2]*Institute of Earth Sciences, The Hebrew University of Jerusalem, Jerusalem 91904, Israel*
[3]*Commonwealth Scientific and Industrial Research Organization, Exploration and Mining, Kensington, WA 6151, Australia*

ABSTRACT

Following the Neoproterozoic Pan-African orogeny, the Arabian-Nubian Shield of North Africa and Arabia was eroded and then covered by Cambrian sandstones that record the onset of platform sedimentation. We applied K-feldspar $^{40}Ar/^{39}Ar$, zircon and apatite fission-track, and apatite (U-Th)/He thermochronology to detritus from Cambrian sandstones of southern Israel deposited at ca. 500 Ma. U-Pb detrital zircon ages from these sandstones predate deposition and record the earlier Neoproterozoic crustal evolution of the Pan-African orogens. $^{40}Ar/^{39}Ar$ ages from 50 single grains of K-feldspar yield a Cambrian mean of ca. 535 Ma. The $^{40}Ar/^{39}Ar$ age spectrum of a multi-grain K-feldspar aliquot displays diffusion behavior compatible with >560 Ma cooling later affected by a heating event. Assuming that the high-temperature domains of the K-feldspars have not been affected by subsequent (hydro)thermal events, and taking previously published K-Ar and Rb-Sr ages from other parts of the East African Orogen at face value, these ages apparently record Pan-African thermal resetting below a thick volcano-sedimentary pile similar to the Saramuj conglomerate in Jordan and/or the Hammamat in Egypt. Detrital zircon fission-track (ZFT) ages cluster around 380 Ma, consistent with previous ZFT results from Neoproterozoic basement and sediments of the region, revealing that the Cambrian platform sequence experienced a middle Devonian thermal event and low-grade metamorphism. Regional correlation indicates that during Devonian time the sedimentary cover atop the Cambrian in Israel was never in excess of 2.5 km, requiring an abnormally steep geothermal gradient to explain the complete ZFT annealing. A basal Carboniferous unconformity can be traced from Syria to southern Saudi Arabia, suggesting that the observed Devonian ZFT ages represent a regional tectonothermal event. Similar Devonian ZFT ages were reported from Arabian-Nubian Shield basement outcrops in the Eastern Desert, 500 km south of Eilat. The detrital apatites we studied all have extremely rounded cores suggestive of a distant provenance, but some grains also feature distinct euhedral, U-rich apatite overgrowth rims. Authigenic apatite may have grown during the late Devonian thermal event we dated by ZFT, coinciding with existing Rb-Sr ages from authigenic clays in the same deposits and leading to the conclusion that the Devonian event was probably hydrothermal. Like the ZFT ages, the detrital apatite fission-track (AFT) ages were also completely reset after deposition. Sixty single-grain detrital AFT ages group at ca. 270 Ma with significant dispersion. Inverse modeling of the AFT data indicate extended and/or repeated residence in the AFT partial annealing zone, in turn suggesting an episodic burial-erosion history during the Mesozoic caused by low-amplitude vertical motions. Seven detrital apatite (U-Th)/He ages scatter between 33 and 77 Ma, possibly resulting from extreme compositional zonation associated with the authigenic U-rich overgrowths. The ca. 70 Ma (U-Th)/He ages are more likely to be accurate, setting 1–2 km as an upper limit (depending on the geothermal gradient) on the post-Cretaceous exhumation of the Cambrian sandstone and showing no evidence for substantial denudation related to Tertiary rifting of the Red Sea.

†E-mail: p.vermeesch@ucl.ac.uk

Regional Geological Setting

Cambrian sandstones in southern Israel are characteristic of a widespread platform sedimentary cover overlying the Precambrian basement of North Africa and Arabia. Much of the area that formerly constituted the northern margin of Gondwana was shaped by metamorphism, deformation, and igneous activity during the Neoproterozoic Pan-African orogeny (Stern, 1994, and references therein). The assembly of the Gondwana supercontinent during the Neoproterozoic to Early Paleozoic was the consequence of a prolonged history of orogenic amalgamation involving continental fragments from eastern and western Gondwana (e.g., Stern, 1994; Shackleton, 1996, Condie, 2003; Meert, 2003; Collins and Pisarevsky, 2005). The East African Orogen extends from the Arabian-Nubian Shield, along the northern sector into East Antarctica (Stern, 1994; Jacobs and Thomas, 2004) (Fig. 1). It was recently understood that amalgamation of Gondwana occurred during two major periods of orogeny (Meert, 2003; Collins and Pisarevsky, 2005): the pre–600 Ma East African Orogeny and the subsequent 570–500 Ma Kuunga-Malagasy Orogeny. The latter was mainly documented in eastern Madagascar (Collins and Pisarevsky, 2005) as well as in southeast Kenya (Hauzenberger et al., 2007) and eastern Tanzania (Rossetti et al., 2008). Deposition of the Cambrian cover sandstone heralds erosion of the Pan-African orogen and the cratonization of Neoproterozoic mobile belts (Avigad et al., 2003). Platform sedimentation in north Gondwana lasted nearly 500 million years (Alsharhan and Nairn, 1997) but was punctuated by long wavelength vertical motion and a number of unconformities, by Triassic-Jurassic foundering of the Eastern Mediterranean basin (Garfunkel and Derin, 1985), and by Tertiary breakup along the Red Sea–Dead Sea fault system.

GSA Bulletin; July/August 2009; v. 121; no. 7/8; p. 1204–1216; doi: 10.1130/B26473.1; 10 figures; Data Repository item 2009025.

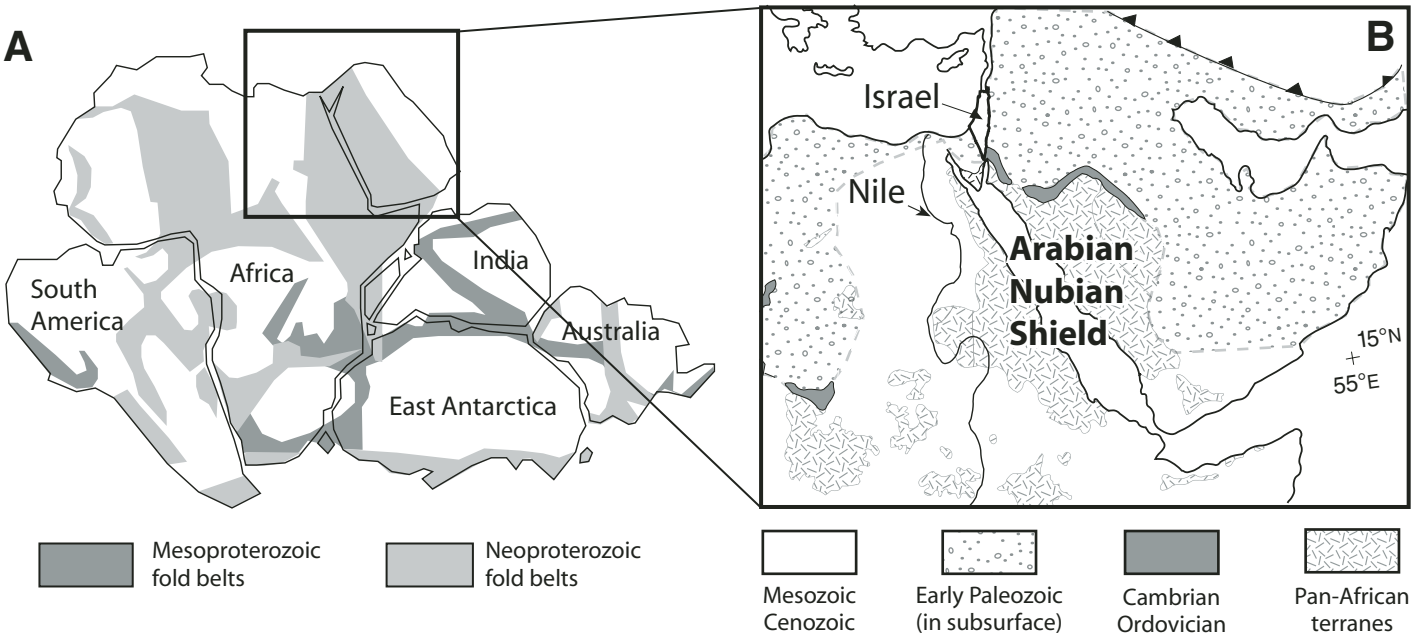

Figure 1. (A) Reconstruction of Gondwana at 500 Ma with indication of the major fold belts (after Unrug, 1997). (B) Geologic map of northeast Africa and Arabia showing exposures of the Precambrian rocks and Paleozoic sediments, modified after Avigad et al. (2003).

During the early Paleozoic, Israel was located near the northern edge of Gondwana at the northern tip of the Arabian-Nubian Shield. The Arabian-Nubian Shield of North Africa and Arabia is a collage of accreted Neoproterozoic island arcs squeezed between east and west Gondwana fragments around 630 Ma (Johnson and Woldehaimanot, 2003; Katz et al., 2004). Current exposure of the northern Arabian-Nubian Shield is dominated by widespread late- to post-orogenic batholiths intruded at 630–600 Ma (Bentor, 1985, and references therein). Calc-alkaline magmatism was followed by a major phase of erosion, extension, and alkaline igneous activity at around 600–580 Ma (Beyth et al., 1994; Garfunkel, 1999). Various Rb/Sr and K-Ar studies have suggested that igneous activity may have lasted until 540 Ma (Bentor, 1985; Ibrahim and McCourt, 1995; Beyth and Heimann, 1999; Garfunkel, 1999), but this has not been verified by U-Pb zircon geochronology. The youngest U-Pb zircon age in the northern Arabian-Nubian Shield is ca. 580 Ma (Meert, 2003). By Middle Cambrian time, the northern part of the Arabian-Nubian Shield (including southern Israel) was eroded to sea level, and the exhumed basement was subjected to intense weathering. In a world without land plants and under acidic atmospheric conditions, physical and chemical weathering attacked the freshly exhumed basement, and a system of braided rivers deposited vast sheets of Cambro-Ordovician "Nubian sandstone" (Weissbrod, 1980; Weissbrod and Nachmias, 1986; Avigad et al., 2005). The weathered basement was progressively blanketed (from north to south; e.g., Garfunkel, 1999) and the entire Arabian-Nubian Shield as far south as Ethiopia and Yemen was covered by a siliciclastic veneer by Ordovician time (Garfunkel, 2002; Kolodner et al., 2006). Continuous sedimentation in the Levant continued until Late Devonian time, when the sedimentary cover reached a thickness of ~2.5 km (Garfunkel and Derin, 1985; Gvirtzman and Weissbrod, 1985; Segev et al., 1995). Hercynian doming interrupted Paleozoic sedimentation, and a regional unconformity marks the base of the Carboniferous (Gvirtzman and Weissbrod, 1985). The area was later affected by the Triassic to Early Jurassic opening of the Eastern Mediterranean basin (Garfunkel and Derin, 1985). Thick wedges of predominantly marine sediments, including substantial amounts of carbonate, were deposited on the subsiding passive margin until the Late Cretaceous, when tectonism affected the northern and eastern margins of the Arabian-Nubian Shield (Garfunkel and Derin, 1985). Miocene-Oligocene opening of the Red Sea was initially accommodated by rifting in the Gulf of Suez, but at 4–5 Ma, plate motion shifted to the left-lateral Dead Sea transform fault (Bartov et al., 1980). Approximately 105 km of strike-slip motion (Quennell, 1958) formed several pull-apart basins, of which the Dead Sea is the largest (Garfunkel and Ben-Avraham, 1996). We applied low-temperature thermochronology to platform detritus from southern Israel to learn about events that affected the lithosphere before and after their deposition in the Cambrian. Our results illuminate the final stages of Neoproterozoic to Cambrian Pan-African orogeny in this region and help to monitor the long-term, post-depositional thermal evolution of the siliciclastic platform deposits.

The Cambrian of Southern Israel

Cambrian strata in southern Israel near Eilat overlie the Neoproterozoic basement of the Arabian-Nubian Shield (Weissbrod, 1980; Weissbrod and Nachmias, 1986), which was exposed in the Gulf of Eilat and Sinai in the Tertiary as a result of breakup and rifting along the Red Sea. The Cambrian section at Eilat can be correlated with similar sections across the Dead Sea rift in Jordan, which in turn can be linked to exposures farther east and southeast in Saudi Arabia (e.g., the lower part of the Saq Formation; Powers et al., 1966). At Eilat, the 300 m Cambrian section gradually changes upward from subarkose to mature quartz arenite (Fig. 2). Fluvial deposits are common at the base, shallow marine sandstones dominate the remainder, and shale and carbonate are present locally. From base to top, the Cambrian sequence in the Eilat area includes (Weissbrod, 1980; Segev, 1984; Garfunkel, 2002):

(1) *Amudei Shelomo Formation*—made of relatively immature arkose and subarkose overlying deeply weathered Neoproterozoic basement. A basal polymictic conglomerate is often present.

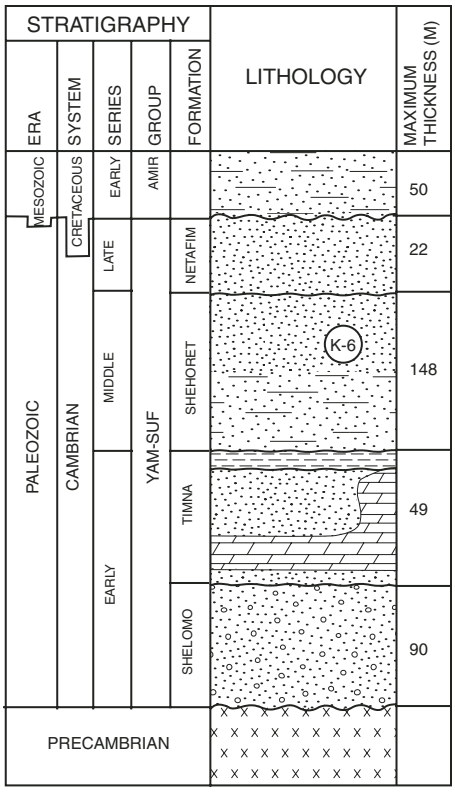

Figure 2. Stratigraphic section of the Cambrian of southern Israel. The deeply weathered Late Proterozoic granitoid basement is unconformably overlain by lower Cambrian pebbly arkoses of the Shelomo Formation, subarkoses and carbonates of the Timna Formation, and fine-grained subarkoses and quartz-arenites of the Shehoret and Netafim Formation (redrafted from Segev, 1984).

(2) *Timna Formation*—made of mainly subarkose with local carbonate facies. Scarce trilobites in the carbonates (Parnes, 1971) indicate that these rocks and the overlying parts of the section are younger than 520 Ma (e.g., Landing et al., 1998).

(3) *Shehoret Formation*—consisting of fine- to coarse-grained subarkose.

(4) *Netafim Formation*—comprised of Late Cambrian fine-grained quartz arenite with alternating layers of siltstone and claystone.

(5) *Amir Formation*—made of Lower Cretaceous sandstones unconformably overlying the Cambrian section.

The general trend of increasing sediment maturity is common to the Cambrian section of southern Israel and sections in Jordan, the Sinai, and northern Saudi Arabia (Weissbrod and Nachmias, 1986; Avigad et al., 2005; Kolodner et al., 2006), but the depositional gap represented by the unconformity below the Amir Formation varies. In the subsurface north of Eilat the Cambrian is overlain by Late Carboniferous to Permian sandstones, whereas in southwestern Sinai, the Cambrian is overlain by Carboniferous sediments (Weissbrod, 1980; Garfunkel 2002). A more complete lower Paleozoic section is preserved in Jordan and northern Saudi Arabia, where continuous sedimentation occurred from Cambrian to Devonian time (Fig. 2 of Weissbrod and Nachmias, 1986, and references therein). These geologic constraints are important for the interpretation of the data presented later. Deposition of Late-Middle to Late Cambrian sandstone marks the end of the Pan-African orogeny in the region and the onset of platform sedimentation. Detrital zircon U-Pb geochronology (Avigad et al., 2003; Avigad et al. 2005; Kolodner et al., 2006) revealed that the Cambro-Ordovician sandstones reflect the crustal composition of broad segments of the Arabian-Nubian Shield and beyond it (Kolodner et al., 2006). The Cambro-Ordovician sandstones on the entire North Gondwana margin are mineralogically and often texturally mature (Avigad et al., 2005, and references therein), indicating significant chemical and physical weathering and long-distance transport. The provenance area of the Cambro-Ordovician sandstone was very large, and detritus was transported for hundreds and possibly thousands of kilometers. The Cambro-Ordovician sandstones are thus an excellent monitor of continental-scale geological processes at an important time in Earth history. This study extends the perspectives gained from U-Pb detrital zircon geochronology by applying a suite of thermochronometric techniques to detritus from a fine-grained, subarkose sample of the Shehoret Formation deposited at ca. 500 Ma. We present and discuss new detrital K-feldspar $^{40}Ar/^{39}Ar$ ages, zircon and apatite fission-track ages, and apatite (U-Th)/He ages. Taken together, our new data reveal a lengthy and more detailed picture of the pre- and post-depositional thermal history of the Nubian Sandstone.

METHODS

Sample K-6 was collected from the Shehoret Formation, close to and from the same horizon as sample K-5 of Kolodner et al. (2006) for which detrital zircon U-Pb ages are available (Fig. 3). Because the sample was only weakly consolidated, it was gently crushed by mortar and pestle, thus reducing the potential for damage to apatite grains. After soaking in 10% acetic acid and 3% hydrogen peroxide until reactions ceased, magnetic separation was done by vertical and slope Frantz. The nonmagnetic fraction was placed in lithium metatungstate with a density of 2.96 g/cm^3 to separate quartz and feldspar from apatite and zircon. The light and the heavy fractions were next placed in methylene iodide, with density 2.59 g/cm^3 and 3.3 g/cm^3, respectively, to separate K-feldspar from quartz and plagioclase, and apatite from zircon.

Two aliquots of detrital K-feldspar were prepared for $^{40}Ar/^{39}Ar$ analysis and irradiated at Oregon State University. Neutron flux was monitored by co-irradiating grains of U.S. Geological Survey standard Taylor Creek Rhyolite (TCR) sanidine with an assumed age of 28.34 ± 0.14 Ma (Renne et al., 1998). Upon return from the reactor, one aliquot was unwrapped and 50 single grains were placed in a crucible under high vacuum for laser analysis at Stanford University. Apparent ages (GSA Data Repository Item)[1] of single grains were measured by total fusion with an Ar-ion laser. The second aliquot was analyzed by stepwise heating in a double-vacuum resistance furnace. For both aliquots the gettered gas was analyzed in a high-sensitivity MAP 216 noble-gas mass spectrometer with Baur-Signer ion source (Baur, 1980).

Zircon fission-track ages were measured by Paul O'Sullivan of Apatite to Zircon using the external detector method (Hurford and Green, 1983). Fish Canyon Tuff zircon was used as an irradiation standard. Apatites were mounted in epoxy, ground, and polished. The mounts were etched for 15 s in 23% HNO_3 at 25 °C (Jonckheere et al., 2007). They were then covered with muscovite external detectors and irradiated at the Garching-Munich reactor. The muscovite external detectors were etched in 40% HF for 30 min at room temperature. Two mounts of Fish Canyon apatite and three shards of Durango apatite standards were irradiated together with the sample along with mm-sized shards of standard uranium glass. Track counting was performed at the Swiss Federal Institute of Technology, on c-axis parallel apatite surfaces under 1250× magnification. The muscovite external detectors were repositioned trackside down on the apatite mounts in the same position as during irradiation. Fossil tracks were counted by focusing on the apatite surface through the muscovite detector; induced tracks were counted by focusing on the underside of the external detector without moving the microscope stage (Jonckheere et al., 2003). Chlorine content was used as the kinetic parameter and measured on a Jeol 8100 electron microprobe at Birkbeck, University of London. Analysis was carried out using an accelerating

[1]GSA Data Repository item 2009025, $^{40}Ar/^{39}Ar$, fission track and (U-Th)/He data, is available at http://www.geosociety.org/pubs/ft2008.htm or by request to editing@geosociety.org.

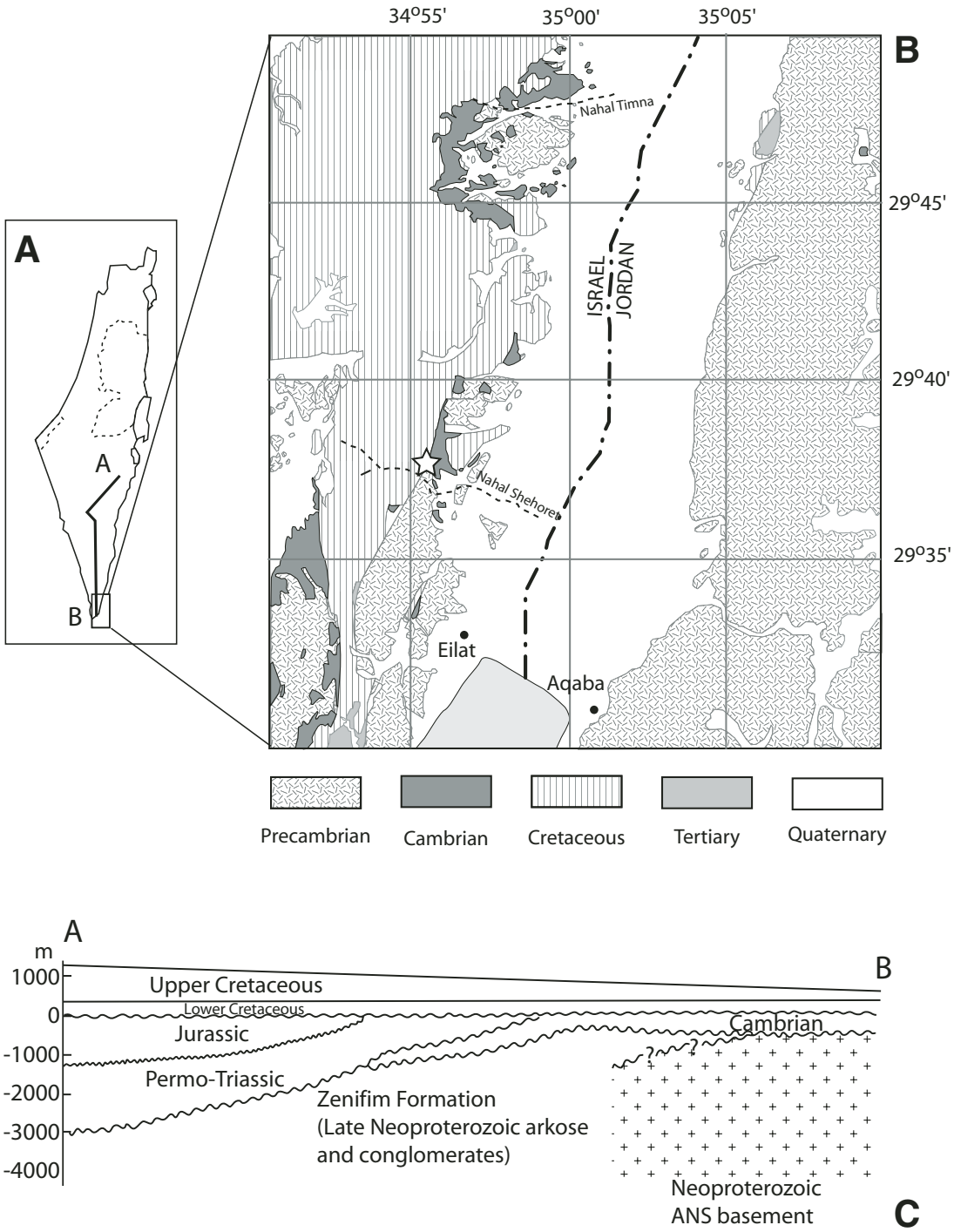

Figure 3. (A) Map of Israel with indication of the field area. (B) Location map of samples K-5 and K-6, indicated by the star. Modified from Sneh et al. (1998). (C) Schematic stratigraphic section of southern Israel with indication of the major unconformity (redrafted from Kohn et al., 1992). Abbreviation: ANS—Arabian-Nubian Shield.

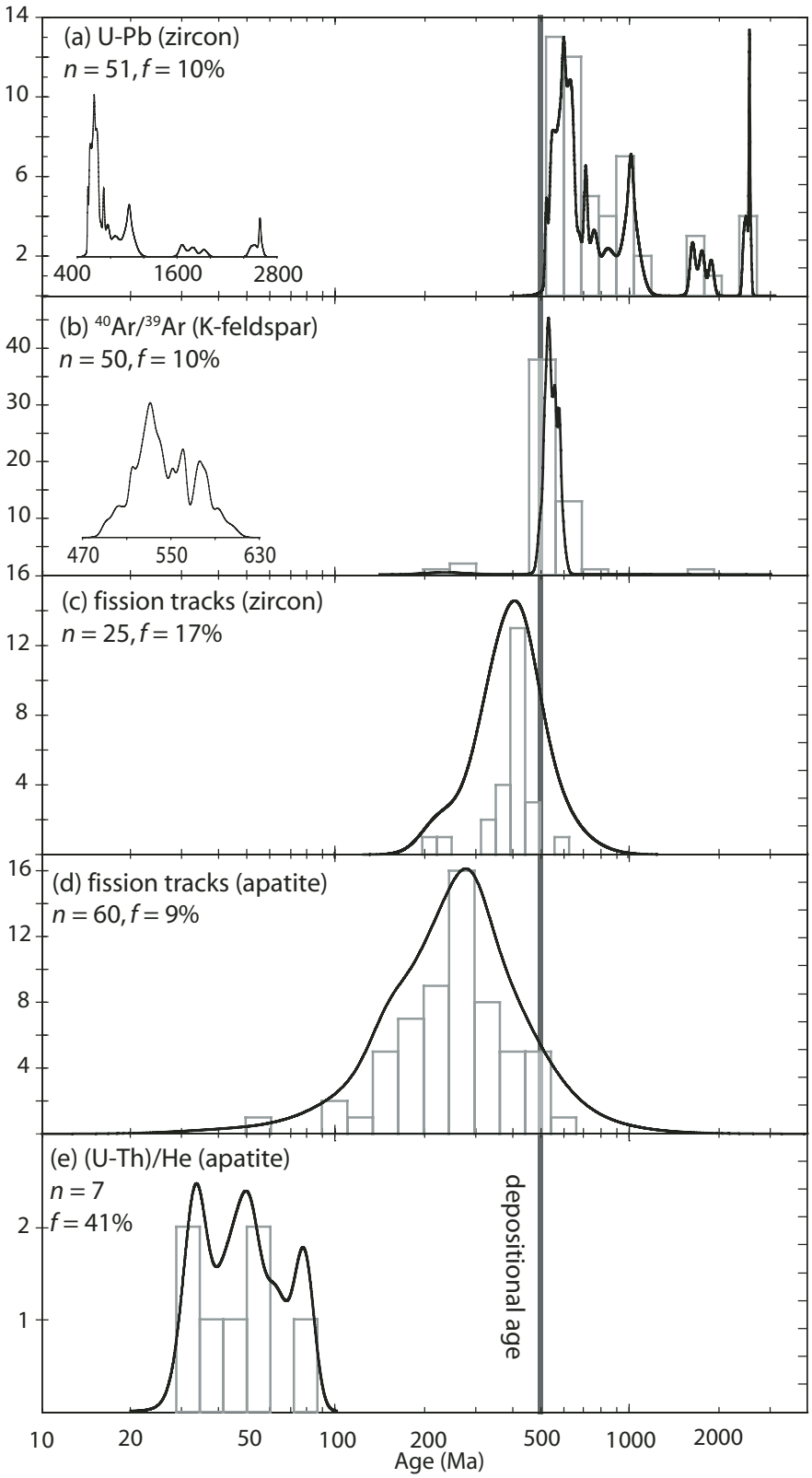

Figure 4. Detrital grain-age histograms and density estimates of (A) zircon U-Pb, (B) K-feldspar $^{40}Ar/^{39}Ar$, (C) zircon fission tracks, (D) apatite fission tracks, and (E) apatite (U-Th)/He data. Note the logarithmic scale on the time-axis of the main graph, a linear version of the high-temperature data is shown as insets. Abbreviations: *n*—number of grains; *f*—smallest fraction sampled with >95% certainty (Vermeesch, 2004).

voltage of 15 kV, current of 2.5 nA, and a beam diameter of 1 µm. The analyses were calibrated against standards of natural silicates, oxides, and Specpure® metals with the data corrected using a ZAF program.

Apatite grain dimensions were measured by a binocular microscope at 200× magnification. The alpha-retention factor F_t was calculated from the surface-to-volume ratio of the grains (Meesters and Dunai, 2002) using an ellipsoidal approximation that was more appropriate to the shape of our detrital apatites (see discussion later). Helium was extracted in a 3 min laser heating using a 1064 nm wavelength Nd-YAG laser. Reextraction yielded no detectable helium, indicating complete degassing. The evolved gas was cleaned in a liquid N_2-cooled, activated charcoal, cold-finger and Ti/Zr and Al/Zr getters. ^{4}He was measured by peak-height calibration to a known amount of ^{4}He in a custom-built, sector-type mass spectrometer at the Swiss Federal Institute of Technology. After He extraction, the Pt packets were recovered from the laser pan, partially opened under the binocular microscope, and placed in Teflon vials. The samples were spiked with ~50 fmol of ^{233}U and ~20 fmol of ^{229}Th. Approximately 1 ml of concentrated high-purity, quartz-distilled HNO_3 was added. After digestion on a hot plate (~150 °C) for 24 h, the HNO_3 was evaporated, and ~1 ml of a 6% HNO_3–0.8% HF solution was added. ^{229}Th, ^{232}Th, ^{235}U, and ^{238}U were measured in low mass resolution by single-collector, inductively coupled plasma–sector field–mass spectrometry (ICP-SF-MS) (Element2).

RESULTS

Previously Published Zircon U-Pb Ages

The detrital zircon age spectrum from sample K-5 resembles that of other samples of Cambrian and Ordovician sandstones in Israel and Jordan (Kolodner et al., 2006), providing an image of the pre-depositional history of the source terrane (Fig. 4A). Thirty-four of 55 zircons are of Neoproterozoic Pan-African provenance between 900 and 530 Ma. The U-Pb detrital zircon age spectrum generally overlaps with the history of igneous activity in the Arabian-Nubian Shield that lasted for nearly 300 m.y. spanning much of the Neoproterozoic (Stern, 1994). While the pre-Neoproterozoic zircons have been interpreted as far-traveled, it is possible that some are recycled inherited grains derived from more proximal Neoproterozoic rocks (Avigad et al., 2003; Hargrove et al., 2006). The precise origin of Late Neoproterozoic to Cambrian age (570–530) detrital zircons is also not known because potential source rocks displaying U-Pb zircon

ages of this type are uncommon in the northern Arabian-Nubian Shield (Meert, 2003). Such rocks are more common in the southern half of the East African Orogen (Küster and Harms, 1998) and are plausible sources because the textural and mineralogical maturity of the sandstone evinces significant transport. Five grains are actually younger than the inferred 500 Ma depositional age of the Shehoret Formation, and three of these five are concordant. We are confident that these anomalously young ages are not a result of sample contamination because the four samples studied by Kolodner et al. (2006) from the Shehoret area contained a similar proportion of anomalously young grains. Later in this paper we will propose an authigenic origin for these zircons.

K-Feldspar $^{40}Ar/^{39}Ar$ Ages

Two sets of $^{40}Ar/^{39}Ar$ data were collected from sample K-6. Fifty single-grain, K-feldspar, laser total-fusion extractions yielded a population of ages that tightly cluster around 535 Ma (Cambrian), indicating a single provenance and thermal history. About half of these grains yield apparent ages that are younger than the zircon U-Pb age spectrum, whereas the other half overlap with the very latest phase of igneous activity as recorded in the zircon U-Pb age spectra. Nearly all K-feldspar grains are older than the depositional age, although some by only a few million years (Fig. 4B). A similar picture emerges from the step-heating experiment (Fig. 5). Except for the first few temperature steps that amount to less than 10% of the ^{39}Ar released, the spectrum yields late Neoproterozoic to Cambrian apparent ages between 520 and 580 Ma. Because it is possible that even the high-temperature part of the age spectrum is affected by hydrothermal alteration, these should be considered minimum ages. The Arrhenius diagram shows multi-diffusion–domain behavior typical of K-feldspars (Fig. 5). The short time lag between the $^{40}Ar/^{39}Ar$ ages and the depositional age of the sandstone suggests that these grains cooled rapidly, an observation that is corroborated by the step-heating experiment. Because K-feldspars cannot be characterized by a single-diffusion domain, they rarely feature easily interpretable age spectra, especially if they experienced a slow and complex thermal history (Lovera et al., 1989). Alternatively, the "kink" in the Arrhenius diagram could also be an artifact of multiple stages of crystal growth (Villa, 2006). In this context, the relatively flat age spectrum of K-6 can be taken as evidence for the simple, rapid, and quasi-simultaneous cooling and/or crystallization of all the K-feldspar grains contained in it. The flat appearance of the age spectrum also lends credibility to the single-step, total-fusion ages of the detrital K-feldspar grains (Lovera et al., 1999). The "partial retention zone" of the $^{40}Ar/^{39}Ar$ system in K-feldspar is between 200 and 400 °C for cooling rates greater than 5 °C/Ma (Lovera et al., 1993). Because all the detrital K-feldspars and nearly the entire $^{40}Ar/^{39}Ar$ age spectrum are older than the depositional age, the sample was probably not heated to more than 200 °C after deposition, nor did it undergo complete recrystallization. Because the sample was a composite collection of unreset detrital grains, we did not attempt to extract a continuous time-temperature model from the data by inverse modeling (Lovera et al., 1989). Different grains within the sample went through different high-temperature histories but shared a common low-temperature history. Therefore, the low-temperature part of the step-heating experiment might contain a post-depositional reheating signal, an idea that will be discussed in the following section. The flat section of the age spectrum represents an averaged high-temperature age signal of all the component grains. Thus, the average K-feldspar grain in our sample passed through the 300 °C isotherm before 560 Ma.

Zircon Fission-Track (ZFT) Ages

Fission-track ages are roughly proportional to the ratio of the number of spontaneous tracks to the number of induced tracks, both of which have a Poisson distribution. Because the logarithm of the ratio of two Poisson-distributed quantities has an approximately Gaussian distribution, the data of Figure 4 are shown with a logarithmic time axis (Brandon, 1996). The ZFT ages tightly cluster around 380 Ma (Late Devonian), substantially younger than the depositional age and suggest a significant post-depositional thermal event.

Apatite Fission-Track (AFT) Ages

Sample K-6 contained extremely rounded apatites (Fig. 6A). Morphological and compositional details of these grains are visible in Figure 6. About 20% of the detrital apatites feature distinct overgrowths of euhedral apatite (Figs. 6A and 6B). The fission tracks induced in the muscovite external detector reveal that these overgrowths are richer in uranium than their rounded cores (Fig. 6C). The spread of the AFT ages is substantially greater than that of the ZFT ages (Fig. 4D) because of the lower number of tracks in the apatite. There are fewer induced tracks because the sample was somewhat under-irradiated (we did not expect to find such old ages), and there are fewer spontaneous tracks because apatite generally has a lower uranium concentration than zircon. The AFT ages approximately follow a lognormal distribution (Fig. 4D) with a median and central age around 270 Ma and an age dispersion (Galbraith, 1990) of 19%. The horizontally confined fission-track length distribution is approximately normally distributed with a mean of 9.3 µm and a standard deviation of 2.3 µm. Electron microprobe analysis revealed that our sample contains almost pure F-apatite. The Cl content is very low (<0.1 wt%), significantly lowering the annealing temperature of our sample (Green et al., 1986).

Apatite (U-Th)/He

Seven apatite grains yielded (U-Th)/He ages between Late Cretaceous and Eocene. As is often the case with (U-Th)/He data, the substantial scatter cannot be explained by the analytical uncertainty of the U, Th, and He measurements alone (Fitzgerald et al., 2006). We postulate that in this case the scatter is caused principally by the alpha-ejection correction, which assumes a uniform chemical composition. As noted above, a substantial number of the apatites in sample K-6 are compositionally zoned (Fig. 6). If the rim is intact, this will lead to an overestimation of the alpha-retention factor F_t (Fig. 7). Conversely, (partial) removal of the rim during the mineral separation can also lead to an underestimated alpha-retention factor F_t because of implanted helium.

DISCUSSION

Geodynamic Implications

Unreset detrital K-feldspar $^{40}Ar/^{39}Ar$ ages are generally interpreted either as representing cooling or crystallization of the source terrane. Igneous evolution in the Arabian-Nubian Shield is thought to have outlasted the latest Neoproterozoic. Many have reported Rb-Sr, K-Ar, and $^{40}Ar/^{39}Ar$ ages in the range of 560 to 530 Ma, and some of these results were interpreted to reflect crystallization (Beyth et al., 1994; Ibrahim and McCourt, 1995; Beyth and Heimann, 1999). In particular, it is commonly thought (e.g., Bentor, 1985) that post-orogenic and/or extension-related alkaline igneous activity (as well as several diking phases and various volcanics) occurred between 600 and 540 Ma (at least in the northern Arabian-Nubian Shield). Our literature survey failed to reveal zircon U-Pb ages in support of this; the youngest published zircon age we found is ca. 580 Ma (Jarrar et al., 1991, 1993; see also summary of Arabian-Nubian Shield geochronological data by Meert [2003]). An extensive summary of available geochronological data provided by Meert (2003) reveals

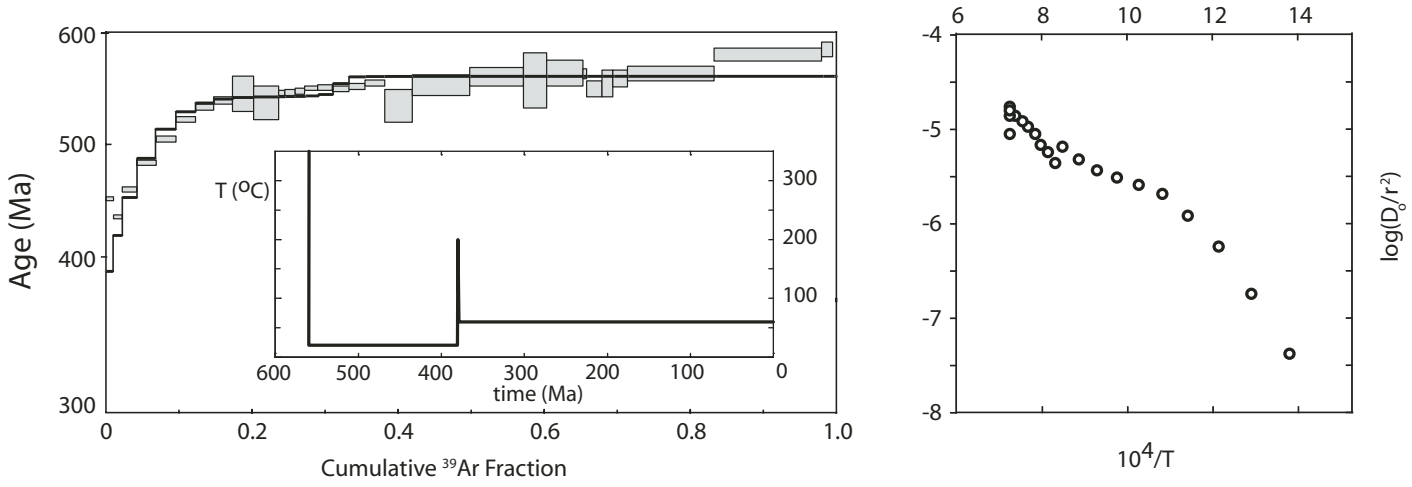

Figure 5. K-feldspar ^{40}Ar/^{39}Ar age spectrum (left, gray blocks) and Arrhenius diagram (right, T <1100 °C). Although the sample consists of unreset detrital grains, and the Arrhenius diagram indicates two diffusion domains, the age spectrum is well behaved, with a "plateau age" of ca. 560 Ma. The low-temperature part of the release spectrum can be replicated (left, black line) by a simple thermal model including a thermal spike to 200 °C at 380 Ma (left, inset). The model was run using SimpleLovera 1.11 (P. Zeitler, Lehigh University) with two diffusion domains (activation energy E_a = 44.21 kcal/mol for both domains; frequency factors $\log_{10}(D_o/a^2)$ = 6.5 and 3; and volume fractions = 0.3 and 0.7, respectively).

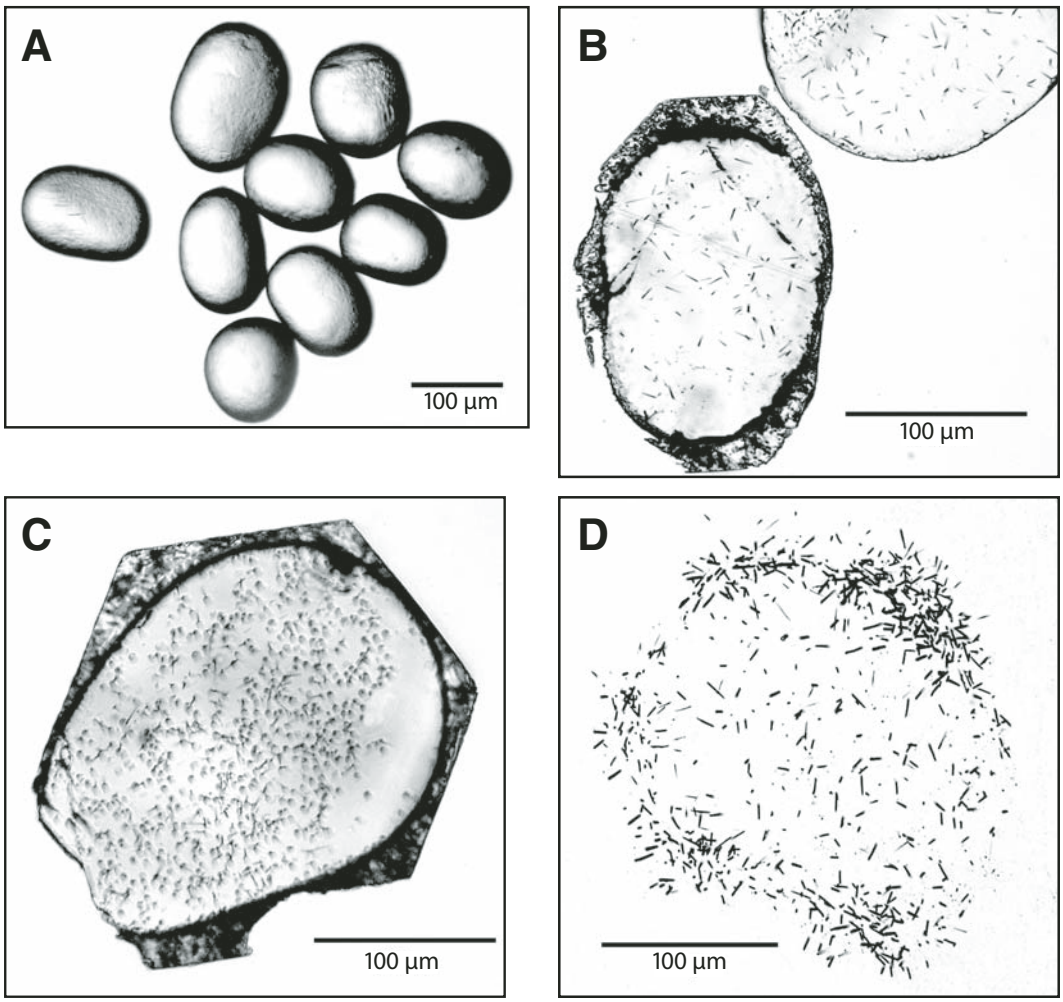

Figure 6. (A) Typical detrital apatite grains from the Shehoret formation, photographed under a binocular microscope in plain light. The rounded shape of the grains indicates that they are far-traveled. (B) Photomicrographs of the fission-track slide, showing detrital apatites with (lower left) and without (upper right) authigenic overgrowth; (C) basal section showing the hexagonal crystal shape of the overgrowth; and (D) the mica print (mirror image) of the same grain shows that the overgrowth is more U-rich than the detrital core.

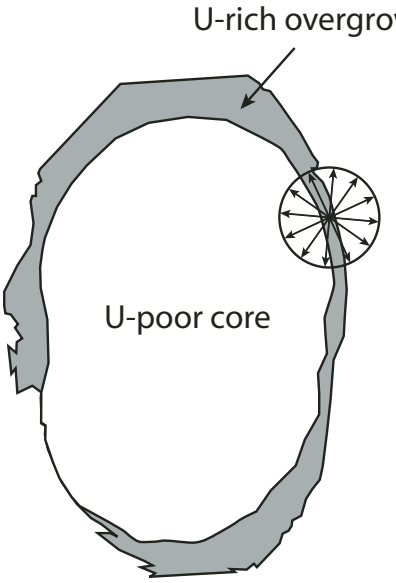

Figure 7. Line-drawing of the apatite with authigenic overgrowth of Figure 6B. Because the overgrowth is richer in U than the detrital apatite core, the conventional alpha-ejection correction is too small. On the other hand, if the U-rich rim has been accidentally removed during mineral separation (bottom left part of the grain), implanted helium from the rim will result in an overestimation of the alpha-ejection correction. α-range—20 μm (radius of the circle).

that U-Pb zircon crystallization ages younger than 580 Ma are confined to the Kuunga-Malagasy Orogen which flanks the Arabian-Nubian Shield in the SE at a distance of some 2000 km from Eilat. Avigad et al. (2003) and Kolodner et al. (2006) demonstrated the presence of far-traveled, pre-Neoproterozoic detrital zircons in Eilat, and it is plausible that the ca. 550 Ma detrital zircons in this area are sourced from such a distal provenance. However, it is unlikely that the detrital K-feldspar in the Shehoret Formation has a similarly distal provenance. With respect to Eilat, a mid to short range provenance within the Arabian-Nubian Shield is the most likely source for these feldspars. Moreover, although some alkaline rocks in southern Israel yielded Rb/Sr ages of ca. 530 Ma, U-Pb dating of an alkaline granite from a nearby outcrop yielded ca. 610 Ma (Beyth et al., 1994). Thus, the interpretation of the 530–560 Ma Rb/Sr and $^{40}Ar/^{39}Ar$ ages in terms of crystallization is questionable. Similar ages in the range of 530 to 540 Ma were reported from many basement rocks of the Arabian-Nubian Shield and were shown to reflect widespread thermal resetting at the end of the Pan-African orogeny. Resetting of the K-Ar and Rb-Sr systems at around 530 Ma in older basement rocks has been reported from the Sinai peninsula (e.g., Bielski et al., 1979; Ayalon et al., 1987), Jordan, Israel, and other parts of the Arabian-Nubian Shield (for example, Fleck et al., 1976) and is one of the most fundamental features of the so-called "Pan-African orogeny" of Kennedy (1964).

It is certainly possible that our K-feldspar $^{40}Ar/^{39}Ar$ ages have been affected by subsequent (hydro)thermal activity and are, therefore, minimum ages. However, in light of the regionally abundant 560–530 Ma cooling ages discussed in the previous paragraph, we should also consider the alternative possibility that our $^{40}Ar/^{39}Ar$ ages are "real." We will make this assumption for the remainder of this section. Because none of the basement rocks exposed in Israel, Jordan, and Sinai yielded zircon U-Pb ages younger than 580 Ma, it is difficult to interpret the K-feldspar ages as crystallization ages. Only the oldest ages in the detrital $^{40}Ar/^{39}Ar$ age spectra could potentially reflect crystallization because they overlap with known crystallization ages defined by U-Pb zircon data. It is more likely that many of the detrital K-feldspars were derived from rocks that were affected by the widespread thermal resetting at the end of Pan-African orogeny. We suggest that insights as to how Arabian-Nubian Shield basement rocks were reset can be obtained from the petrographical observations of sandstone sample K-6. The detritus in this sample is a mixture of subrounded and angular grains reflecting mixing between proximal and more distal provenance. Microcline is the most abundant feldspar in sample K-6. Plagioclase and perthite are practically absent, a feature which is suggestive of elimination of the less resistant minerals by weathering. Furthermore, the exclusive presence of microcline in the sample we dated may be a clue to the geodynamic significance of the Pan-African resetting.

The Pan-African orogeny in the Arabian-Nubian Shield culminated in the intrusion of massive calc-alkaline granitoid batholiths (630–600 Ma; Bentor, 1985; Beyth et al., 1994; Garfunkel, 1999) which currently make up more than 60% of Arabian-Nubian Shield exposure (Stern and Hedge, 1985). Emplacement of these batholiths was immediately followed by intrusion of shallow alkaline granitoids and dike swarms. Petrological observations indicate that the calc-alkaline phase is dominated by subsolvus granitoids featuring Na-rich plagioclase and microcline as individual phases indicating consolidation at significant depth (Garfunkel, 1999). In contrast, the alkaline rocks are shallow-level intrusions, and their mineralogy is often (but not exclusively) dominated by perthite. Because perthite is practically absent from sample K-6, and because calc-alkaline granitoids are by far more abundant, many (if not all) of our $^{40}Ar/^{39}Ar$–dated feldspars were probably derived from the calc-alkaline batholiths. A large body of evidence suggests that calc-alkaline rocks were first exposed by ca. 600 Ma. Neoproterozoic molasse basins formed in the northern Arabian-Nubian Shield immediately following the calc-alkaline batholitic stage. They are well known in Jordan (Saramuj; Jarrar et al., 1993), the Eastern Desert of Egypt (Hammamat; Willis et al., 1988) and in the subsurface of Israel (Zenifim; Weissbrod and Sneh, 2002). They contain immature detritus and conglomerates derived from exposed calc-alkaline granitoids and older basement rocks, and are frequently interbedded with volcanics. The deposition of the Hammamat and hence exhumation of the underlying basement including the abundant calc-alkaline batholiths is constrained by the intrusion of a ca. 585 Ma, perthitic biotite-granite into the sediments (Willis et al., 1988) and by the presence of 600–580 Ma andesites and rhyolites (Dokhan volcanics) interbedded in this unit (Stern and Hedge, 1985). In southern Jordan, the Saramuj Formation is a thick conglomerate unit derived from the underlying basement (Jarrar et al., 1991) and pierced by a ca. 590 Ma monzogranite (Jarrar et al., 1993). Thus, field relations and geochronology indicate that the molasse basins were established upon, and fed from, eroded calc-alkaline batholiths whose ages are no younger than ca. 585 Ma. The observation that the detrital microclines yield 530–560 Ma $^{40}Ar/^{39}Ar$ apparent ages implies that the calc-alkaline source was reheated before exposure and then rapidly cooled. The biotite $^{40}Ar/^{39}Ar$ system in the calc-alkaline basement at Eilat was not reset (620 ± 10 Ma; Cosca et al., 1999), placing tight constraints on the maximum temperature of K-feldspar resetting at 300–350 °C.

Because the calc-alkaline rocks were exposed by ca. 590 Ma, the resetting of their K-feldspar at ~300 °C must have been caused by reburial. Thrust faulting affected segments of the Arabian-Nubian Shield in the Eastern Desert subsequently to the intrusion and exposure of the calc-alkaline granitoids (Greiling et al., 1994; de Wall et al., 2001) and may have caused reburial, but it is questioned whether contraction was regionally wide-

spread. We suggest that late Pan-African thermal resetting was additionally caused by a thick volcanic edifice built upon certain Arabian-Nubian Shield domains some time after ca. 590 Ma and later removed by erosion beginning ca. 560 Ma. Considering the elevated geothermal gradient of 50 °C/km, the thickness of the volcano-sedimentary sequence covering the calc-alkaline basement at ca. 560 Ma locally reached 6 km. Remnants of such a thick volcanic edifice are preserved within the Late Neoproterozoic extensional basins such as the Hammamat, which is still loaded with a 1 km volcanic sequence (Dokhan) whose base locally bears evidence for low-grade metamorphism (Greiling et al., 1994). Given complete exposure of reset basement by 500 Ma (the estimated age of deposition of Shehoret Formation) the postulated ~6 km thick volcanic section was eroded in >60 m.y.

POST-DEPOSITIONAL THERMAL AND BURIAL HISTORY

The ZFT partial annealing zone is 175–250 °C depending on the thermal history (Brandon et al., 1998). Our ZFT ages cluster at 380 Ma, ~100 m.y. younger than the K-feldspar ages and indicating that the Cambrian sandstone section in southern Israel was heated to temperatures corresponding to low-grade metamorphism subsequent to deposition. Although the ZFT data fail the χ^2 test ($P[\chi^2] = 2\%$), the fact that all zircon grains are younger than the depositional age, and the remarkable coincidence between the ZFT ages and authigenic clays in the same deposits (discussed later) indicates that the ZFT system is almost, if not completely, reset. The fact that the ZFT ages are thermally reset whereas the $^{40}Ar/^{39}Ar$ are not implies that the low-grade metamorphism that affected the Cambrian sandstone during Devonian time did not reach temperatures high enough to completely reset the $^{40}Ar/^{39}Ar$ clock of the detrital K-feldspars. It may seem odd that the ZFT thermochronometer is completely reset by a thermal pulse that has only a minor effect on the K-feldspar $^{40}Ar/^{39}Ar$ system. However, the effective closure temperature of the ZFT system is controversial and has been demonstrated to be sensitive to a range of factors, including cooling rate and radiation damage (Brandon et al., 1998; Rahn et al., 2004). Although the combination of these parameters remains poorly understood, the argon and ZFT data nevertheless put tight constraints (within a few tens of degrees) on the post-depositional thermal history of the Shehoret Formation. While we did not attempt to inverse-model the argon release spectrum for the reasons outlined above, we did forward-model a thermal history in which rapid cooling at 560 Ma is followed by a 1 m.y. heating spike to 200 °C at 380 Ma (Fig. 5). Despite its simplicity (only two diffusion domains were employed) the model adequately replicates the low-temperature part of the $^{40}Ar/^{39}Ar$ age spectrum (Fig. 5). Although this model is far from unique (the intensity of the heating peak, for example, could be higher if its duration were shorter), it does illustrate that a single heating pulse could be responsible for the partial loss of radiogenic argon from the least retentive parts of the K-feldspars, while leaving the more retentive zones, which are probed by the high-temperature steps of the release spectrum, largely unaffected.

The late Devonian ZFT ages are entirely compatible with the regional geologic context. By itself, the erosional unconformity between the Late Cambrian Netafim Formation and the Early Cretaceous Amir Formation in southern Israel is not very informative. Tighter constraints are possible if we assume that the northern Arabian-Nubian Shield behaved as a single block and that stratigraphic sections of southern Israel, the Sinai, southern Jordan, and northwestern Saudi Arabia can be reliably correlated (Weissbrod and Nachmias, 1986). In the southwestern Sinai, the Netafim is Early Carboniferous, not Cretaceous, and northwestern Saudi Arabia shows a continuous stratigraphic section from the Cambrian until the Devonian (Fig. 2 of Weissbrod and Nachmias, 1986). Jointly considered, these observations imply that major erosion occurred at or near the Devonian-Carboniferous boundary, when deepest burial also occurred (Segev et al., 1995).

These conclusions agree with an earlier ZFT study from boreholes in Sinai and southern Israel (Kohn et al., 1992) and basement rocks in the Eastern Desert of Egypt (Bojar et al., 2002). ZFT ages for the Precambrian basement and infra-Cambrian sediments in the subsurface of Israel (Zenifim Formation) are within the range 328–373 Ma, consistent with our results for the Shehoret Formation. Although the lower Paleozoic of southern Israel is less than 300 m thick, Kohn et al. (1992) inferred that the basement must have been covered by a thick sedimentary cover that was rapidly removed during an important late Devonian–early Carboniferous tectonic event. This inference was based on their thermochronometric data and the same regional stratigraphic considerations summarized in the previous paragraph. In addition to counting zircon fission tracks, Kohn et al. (1992) analyzed sphene and found it to be only partially reset. The annealing temperature of sphene is slightly higher than zircon, and thus Kohn et al. (1992) constrained the maximum temperature attained during the Devonian-Carboniferous event to ~225 °C. This is in agreement with our thermochronological findings based on the paired $^{40}Ar/^{39}Ar$–ZFT results (see above). Kohn et al. (1992; see also Summer et al., 1995) obtained similar Devonian ZFT ages from Permo-Triassic sandstones, and they concluded that these are recycled earlier Paleozoic sandstone, predicting that the Cambrian of southern Israel should also have been thermally reset by a 370 Ma event. Our data provide the first direct confirmation of their prediction.

The impact of a Devonian thermal event is imprinted in several other mineralogical systems too. Rb-Sr ages of <2 μm clays within shales and dolostones of the Early Cambrian Timna Formation are identical (365–381 Ma) to the ZFT data, as are K-Ar and Rb-Sr ages of the insoluble residue of manganese nodules that are found in the same formation (Segev et al., 1995). Identical ages were obtained by Harlavan (1992) on clay minerals from the Cambrian section in Israel using $^{40}Ar/^{39}Ar$ geochronology, and Heimann et al. (1995) obtained $^{40}Ar/^{39}Ar$ ages of ca. 378 Ma on altered biotites separated from schistose dikes of the Eilat basement and suggested they reflect the influence of a Devonian hydrothermal system. The apatites in the Shehoret Formation give further morphological evidence for a Late Devonian (hydro)thermal event. The cores of the detrital apatites are extremely rounded (Figs. 6 and 7), suggestive of long transport. The authigenic overgrowths of some grains are euhedral and are therefore post-depositional. No authigenic apatites have been reported in deposits younger than Devonian (Weissbrod and Nachmias, 1986). While it has been postulated that abundant U-mineralization observed in the Cambrian of southern Israel occurred during the Neogene (Segev, 1992), our observations imply that a pulse of authigenic apatite growth from a uranium-rich fluid phase occurred during the late Devonian in conjunction with the thermal event recorded by the ZFT. The maximum thickness of the sedimentary cover that overlies the Cambrian of Israel during Devonian time can be estimated by correlation with Jordan, where it is ~2.5 km thick. It is unlikely that the thermal event recorded by the ZFT was uniquely a consequence of burial, because the overburden was too thin to permit temperatures in the range of 200 °C at its base. We suggest that the thermal event resulted from hydrothermal fluid circulation related to low-grade anchimetamorphic phenomena that caused the abundant recrystallization of clay minerals and mobilized U.

As discussed above, Kolodner et al. (2006) reported a small but significant fraction of concordant post-depositional zircon U/Pb ages from the Cambrian section of southern Israel.

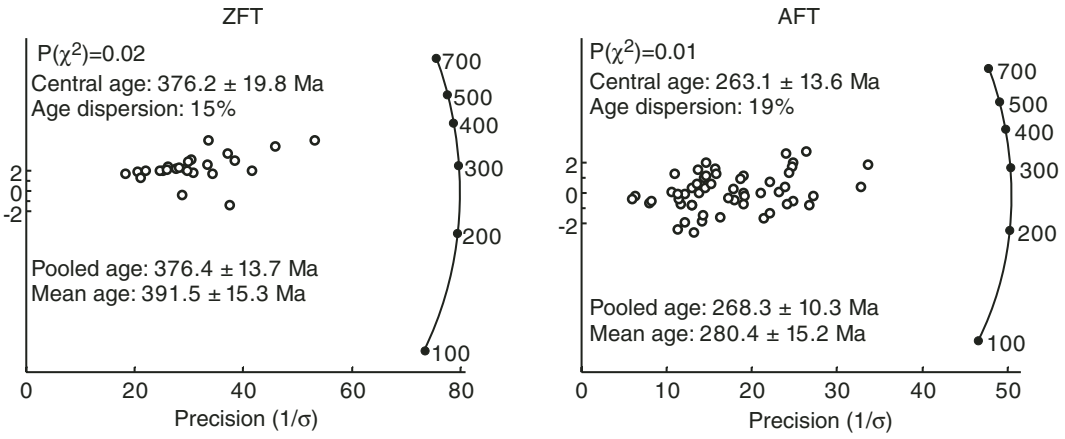

Figure 8. Zircon fission-track (ZFT) and apatite fission-track (AFT) radial plots (Galbraith, 1990).

No such grains were found in the Jordanian sections, which were located 50 km east of our sample (and 100 km south of it, prior to the onset of left-lateral slip on the Dead Sea transform fault). The anomalously young grains are characterized by relatively high U concentrations (Kolodner et al., 2006) and were interpreted as metamict. In view of the U mineralization and the development of U-rich rims around apatites, it is possible that some detrital zircons might have experienced an authigenic overgrowth. Similar observations of authigenic zircon growth have been made elsewhere (Saxena, 1966; Dempster et al., 2004).

Like the zircons, the apatites were also completely reset after deposition. The ca. 270 Ma AFT ages are systematically younger than the ZFT ages by about ~100 m.y. (Figs. 4D and 8). Together with the large spread of the AFT ages, this suggests an extended and/or repeated residence in the AFT partial annealing zone (PAZ: 60–110 °C; Brandon et al., 1998). The unconformity at the base of the Early Cretaceous sandstones that immediately overlie the Cambrian in southern Israel (Fig. 3) is not recorded in the AFT data, implying that probably less than 2 km of sedimentary cover had been eroded by then. As explained previously, the Late Cambrian Netafim Formation in the southwestern Sinai is overlain by Carboniferous deposits. Therefore, there have been at least two episodes of surface exposure of lower Paleozoic rocks in this area. The AFT ages and track-length distribution therefore probably record a complex history with several stages of burial and erosion in and out of the PAZ. In the Eilat area (at the surface) the entire Phanerozoic section (i.e., Cambrian and then Lower Cretaceous to Eocene) is ~1.0–1.2 km thick (Fig. 3C), which is more or less the thickness of the section that was denuded during the Tertiary (Gvirtzman, 2004). Despite the relatively small number (44) of horizontally confined fission tracks in our sample, we inverse modeled the thermal history using the HeFTy program of Ketcham (2005). Chlorine content was used as the kinetic parameter, and default values were used for all settings. The search space was very broadly defined in order to allow nonmonotonic thermal histories. A large number of models were found that can explain the data, all of which indicate a prolonged stay in the upper part of the PAZ (Fig. 9). The models suggest a late Cretaceous heating pulse, consistent with the local stratigraphy and with our (U-Th)/He data, which are discussed next.

The apatite (U-Th)/He ages range from 33 to 77 Ma. The substantial scatter in these data can be explained by the extreme compositional zonation associated with the authigenic U-rich overgrowths on some of the grains. If the overgrowths survived the mineral separation, then the alpha ejection corrections of these grains are too small and the older (U-Th)/He ages (ca. 70 Ma) are more likely to be accurate. With partial retention zone temperatures of ~55–80 °C (Farley, 2000), our (U-Th)/He ages place an upper limit of 1–2 km (depending on the geothermal gradient) on the exhumation of the Shehoret Formation since the Late Cretaceous. We see no evidence for exposure and denudation related to Tertiary Red Sea rifting. This is compatible with the current moderate relief in the vicinity of the Cambrian outcrops near Eilat, on the western side of the Dead Sea transform. Overall, the base of the sedimentary section in southern Israel and the underlying basement were already close to the surface by 70 Ma. Assuming that our apparent (U-Th)/He ages are correct, there is a striking coincidence between them and the apparent heating pulse that clearly stands out from the AFT inverse model (Fig. 10). Because of the imprecision of the latter, it is not clear whether this really reflects a Late Cretaceous tectonic pulse (consistent with Garfunkel and Derin, 1985) or if it coincides with the Tertiary opening of the Red Sea instead. Whatever the underlying cause, the most recent phase in the thermal evolution of the Eilat area is consistent with a decreasing geothermal gradient, as proposed by Kohn et al. (1990).

CONCLUSIONS

This paper illustrates the utility of applying several geochronological and thermochronological techniques to a detrital sample collected from an ancient platform sequence. Together with stratigraphic and petrographic observations, our measurements help create a more detailed picture of the 500 m.y. history of the Late Cambrian Shehoret Formation of southern Israel. Previous U-Pb detrital zircon geochronology of these deposits revealed a mixture of sources and highlighted the Precambrian crustal evolution in the Pan-African provenance, dominated by erosion of the Arabian-Nubian Shield (Kolodner et al., 2006).

Fifty single-grain, K-feldspar, total-fusion argon extractions yielded a population of ages that tightly cluster around 535 Ma (Cambrian). The $^{40}Ar/^{39}Ar$ age spectrum of a multi-grain K-feldspar aliquot displays diffusion behavior compatible with >560 Ma cooling later affected by a heating event. Because our K-feldspar dates are minimum ages, it is certainly possible that the Arabian-Nubian Shield experienced a simple single phase exhumation history during the Neoproterozoic. It is intriguing, however, that similar 560–530 Ma ages have been reported previously in the literature. Although the latter were mostly obtained by the K-Ar and Rb-Sr methods and may, therefore, not be very robust, we did consider the consequences of a 560–530 Ma event for our field area. Our

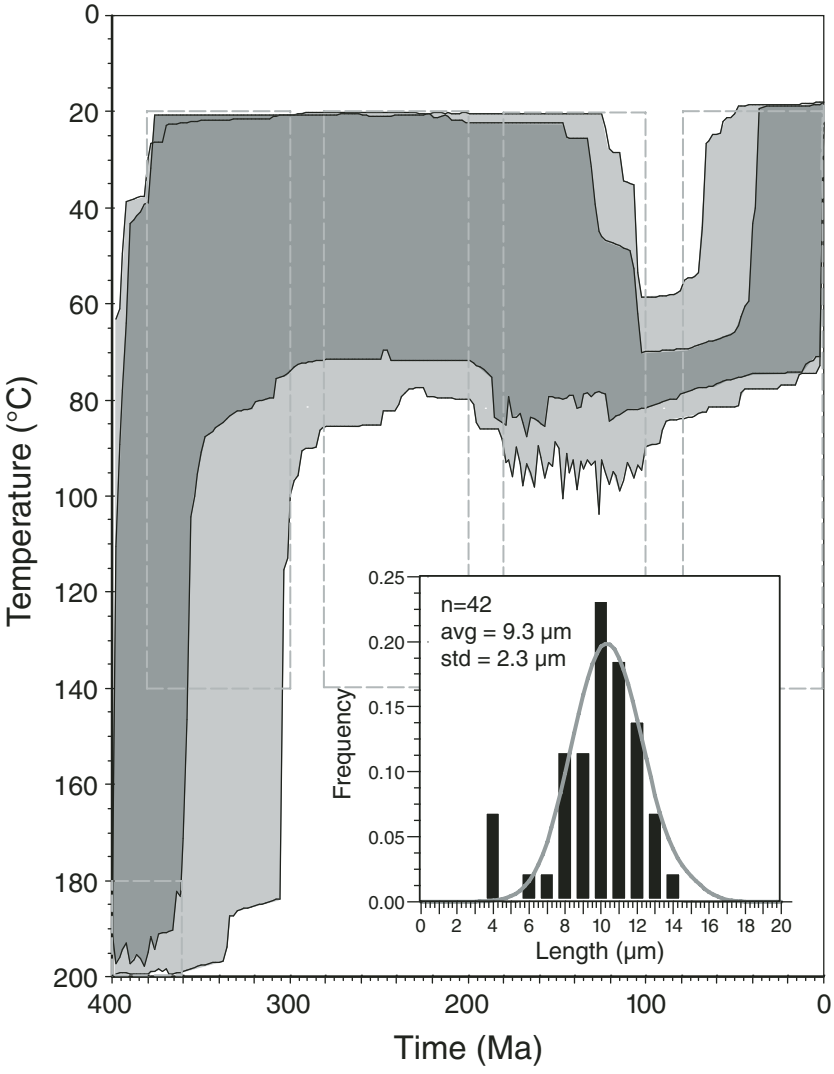

Figure 9. Time-temperature (t-T) diagram obtained by inverse modeling of apatite fission-track (AFT) data using HeFTy (Ketcham, 2005). The inset shows the observed (histogram) and modeled (gray curve) fission-track length distribution.

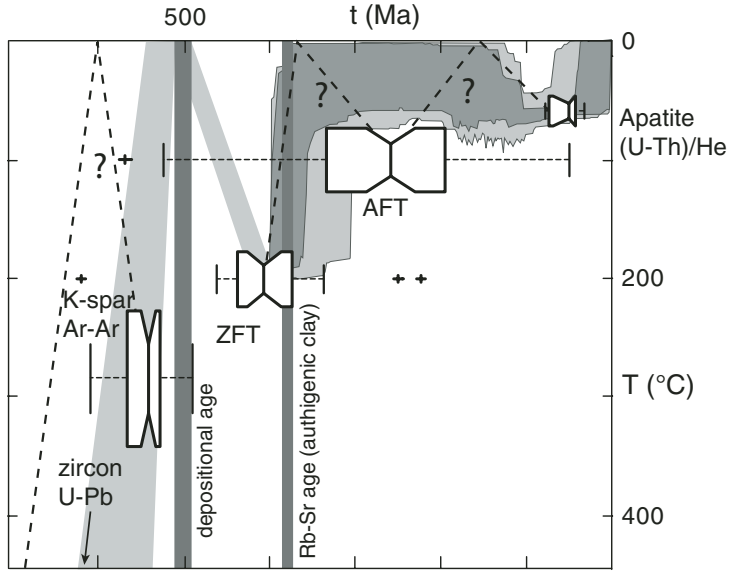

Figure 10. Interpretative time-temperature (t-T) diagram with the thermochronometric data represented as notched box plots (McGill et al., 1978). This diagram shows: rapid cooling and/or reheating of the sediment source area of the Shehoret Formation during the late Proterozoic (ca. 560 Ma); at ca. 380 Ma, the sediments reached their greatest burial depth (~2.5 km; Segev et al., 1995). A hydrothermal event reset the zircon fission-track (ZFT) system and caused the authigenic growth of clays and apatite (Weissbrod and Nachmias, 1986); slow and episodic cooling characterizes post-Devonian times and explains the wide range of apatite fission-track (AFT) ages.

literature survey failed to retrieve U-Pb zircon ages younger than 580 Ma in the northern Arabian-Nubian Shield. Much of the northern Arabian-Nubian Shield crustal surface is dominated by ca. 630 Ma calc-alkaline granites, and it would therefore be likely that many of the detrital K-feldspar grains in the Shehoret formation issued from the erosion of these rocks. Geological evidence (Garfunkel, 1999) indicates that these granitoids were first exposed by ca. 600 Ma. Therefore a preponderance of the 560–530 Ma $^{40}Ar/^{39}Ar$ ages we measured may represent reburial and reheating of Arabian-Nubian Shield crustal segments below a thick volcano-sedimentary pile. The 535–560 Ma ages correspond to Kennedy's "Pan-African event," and although further work is required, this may be the first time the nature of this event has been revealed.

The Cambian-Ordovician sedimentary cover of northern Gondwana was relatively thin (1–3 km thick; Garfunkel, 2002; Kolodner et al., 2006) but covered a very large area from present-day Morocco to Oman (Avigad et al., 2003). The middle Cambrian Shehoret Formation of southern Israel was covered by ~2.5 km of younger sediments by the middle and late Devonian, more than at any other time (Segev et al., 1995). At ca. 380 Ma, a thermotectonic event increased the ambient temperature and heated the Shehoret Formation to ~200 °C, resetting the ZFT system but leaving the K-feldspar $^{40}Ar/^{39}Ar$ system relatively unaffected. Uranium-rich fluids circulated through the sandstone and formed authigenic clays (Segev et al., 1995) and apatite overgrowths (Weissbrod and Nachmias, 1986), which complicate the alpha-ejection correction applied to our apatite (U-Th)/He data. After this fluid circulation event, the Shehoret Formation was repeatedly buried and exhumed in the upper crust (<200 °C), as several regionally important stratigraphic unconformities were created.

AFT inverse modeling confirms this theory and hints at a brief Late Cretaceous to Early Tertiary heating pulse. Although this pulse coincides with seven detrital apatite (U-Th)/He ages, those data show substantial scatter between 33 and 77 Ma, likely resulting from extreme compositional zonation associated with the authigenic U-rich overgrowths. The 70 Ma (U-Th)/He ages are more likely to be accurate, setting 1–2 km as an upper limit (depending on the geothermal gradient) on the post-Cretaceous exhumation of the Cambrian sandstone. Our detrital thermochronology shows no evidence for substantial denudation related to Tertiary rifting of the Red Sea, compatible with the idea that this part of the plate boundary was dominated by strike-slip motion and its western side residing at low elevation.

ACKNOWLEDGMENTS

This paper greatly benefited from constructive reviews by Barry Kohn, Fred Jourdan, Joseph Meert, Zhengxiang Li (Associate Editor), and Karl Karlstrom (Editor). Pieter Vermeesch would like to thank Jim Metcalf for help with the argon measurements; Paul O'Sullivan for the ZFT dating; Eva Enkelmann and Diane Seward for assistance with the AFT dating; and Andy Beard for the electron microprobe measurements. Dov Avigad was funded by the Israel Science Foundation (ISF) grant number 855/06.

REFERENCES CITED

Alsharhan, A.S., and Nairn, A.E.M., 1997, Sedimentary basins and petroleum geology of the Middle East: Amsterdam, Elsevier, 811 p.

Avigad, D., Sandler, A., Kolodner, K., Stern, R.J., McWilliams, M., Miller, N., and Beyth, M., 2005, Mass-production of Cambro-Ordovician quartz-rich sandstone as a consequence of chemical weathering of Pan-African terranes: Environmental implications: Earth and Planetary Science Letters, v. 240, p. 818–826, doi: 10.1016/j.epsl.2005.09.021.

Avigad, D.K.K., McWilliams, M., Persing, H., and Weissbrod, T., 2003, Origin of northern Gondwana Cambrian sandstone revealed by detrital zircon SHRIMP dating: Geology, v. 31, p. 227–230, doi: 10.1130/0091-7613(2003)031<0227:OONGCS>2.0.CO;2.

Ayalon, A., Steinitz, G., and Starinsky, A., 1987, K-Ar and Rb-Sr whole-rock ages reset during Pan African event in the Sinai Peninsula (Ataqa area): Precambrian Research, v. 37, no. 3, p. 191–197, doi: 10.1016/0301-9268(87)90066-0.

Bartov, Y., Steinitz, G., Eyal, M., and Eyal, Y., 1980, Sinistral movement along the Gulf of Aqaba—Its age and relation to the opening of the Red Sea: Nature, v. 285, p. 220–222, doi: 10.1038/285220a0.

Baur, H., 1980, Numerische simulation und praktische Erprobung einer rotationssymmetrischen Ionenquelle für Gasmassenspektrometer [Ph.D. dissertation No. 6596]: Eidgenössische Technische Hochschule Zürich (in German).

Bentor, Y.K., 1985, The crustal evolution of the Arabo-Nubian Massif with special reference to the Sinai peninsula: Precambrian Research, v. 28, p. 1–74, doi: 10.1016/0301-9268(85)90074-9.

Beyth, M., and Heimann, A., 1999, The youngest igneous event in the crystalline basement of the Arabian-Nubian shield, Timna igneous complex: Israel Journal of Earth Sciences, v. 48, p. 113–120.

Beyth, M., Stern, R.J., Altherr, R., and Kröner, A., 1994, The late Precambrian Timna igneous complex, southern Israel: Evidence for comagmatic-type sanukitoid monzodiorite and alkali granite magma: Lithos, v. 31, p. 103–124, doi: 10.1016/0024-4937(94)90003-5.

Bielski, M., Jäger, E., and Steinitz, G., 1979, The geochronology of Ikna granite (wadi Kid pluton), southern Sinai: Contributions to Mineralogy and Petrology, v. 70, p. 159–165, doi: 10.1007/BF00374445.

Bojar, A., Fritz, H., Kargl, S., and Unzog, W., 2002, Phanerozoic tectonothermal history of the Arabian-Nubian shield in the Eastern Desert of Egypt: Evidence from fission track and paleostress data: Journal of African Earth Sciences, v. 34, p. 191–202, doi: 10.1016/S0899-5362(02)00018-0.

Brandon, M.T., 1996, Probability density plot for fission-track grain-age samples: Radiation Measurements, v. 26, no. 5, p. 663–676, doi: 10.1016/S1350-4487(97)82880-6.

Brandon, M.T., Roden-Tice, M.K., and Garver, J.I., 1998, Late Cenozoic exhumation of the Cascadia accretionary wedge in the Olympic Mountains, northwest Washington State: Geological Society of America Bulletin, v. 110, no. 8, p. 985–1009, doi: 10.1130/0016-7606(1998)110<0985:LCEOTC>2.3.CO;2.

Collins, A.S., and Pisarevsky, S.A., 2005, Amalgamatine eastern Gondwana: The evolution of the circum-Indian orogens: Earth-Science Reviews, v. 71, p. 229–270, doi: 10.1016/j.earscirev.2005.02.004.

Condie, K.C., 2003, Tectonics of Rodinia and Gondwana: Continental growth, supercontinent assembly and breakup, *in* Yoshida, M., Windley, B.F., and Dasgupta, S., eds., Proterozoic East Gondwana: Supercontinent assembly and breakup: The Geological Society of London Special Publication 206, p. 1–21.

Cosca, M.A., Shimron, A., and Caby, R., 1999, Late Precambrian metamorphism and cooling in the Arabian-Nubian shield: Petrology and $^{40}Ar/^{39}Ar$ geochronology of metamorphic rocks of the Eilat area (southern Israel): Precambrian Research, v. 98, p. 107–127, doi: 10.1016/S0301-9268(99)00044-3.

Dempster, T.J., Hay, D.C., and Bluck, B.J., 2004, Zircon growth in slate: Geology, v. 32, no. 3, p. 221–224, doi: 10.1130/G20156.1.

de Wall, H., Greiling, R.O., and Sadek, M.F., 2001, Post-collisional shortening in the late Pan-African Hamisana high strain zone, SE Egypt: Field and magnetic fabric evidence: Precambrian Research, v. 107, p. 3–4, 179–194, doi: 10.1016/S0301-9268(00)00141-8.

Farley, K.A., 2000, Helium diffusion from apatite: General behavior as illustrated by Durango fluorapatite: Journal of Geophysical Research, v. 105, no. B2, p. 2903–2914, doi: 10.1029/1999JB900348.

Fitzgerald, P.G., Baldwin, S.L., Webb, L.E., and O'Sullivan, P.B., 2006, Interpretation of (U-Th)/He single grain ages from slowly cooled crustal terranes: A case study from the Transantarctic Mountains of southern Victoria Land: Chemical Geology, v. 225, p. 91–120, doi: 10.1016/j.chemgeo.2005.09.001.

Fleck, R.J., Coleman, R.G., Cornwall, H.R., Greenwood, W.R., Hadley, D.G., Schmidt, D.L., Prinz, W.C., and Ratté, J.C., 1976, Geochronology of the Arabian Shield: Geological Society of America Bulletin, v. 87, p. 9–21, doi: 10.1130/0016-7606(1976)87<9:GOTASW>2.0.CO;2.

Galbraith, R.F., 1990, The radial plot: Graphical assessment of spread in ages: Nuclear Tracks and Radiation Measurements, v. 17, p. 207–214, doi: 10.1016/1359-0189(90)90036-W.

Garfunkel, Z., 1999, History and paleogeography during the Pan-African orogen to stable platform transition: Reappraisal of the evidence from Elat area and the northern Arabian-Nubian Shield: Israel Journal of Earth Sciences, v. 48, p. 135–157.

Garfunkel, Z., 2002, Early Paleozoic sediments of NE Africa and Arabia: Products of continental-scale erosion, sediment transport, and deposition: Israel Journal of Earth Sciences, v. 51, p. 135–156, doi: 10.1560/WE3P-3EX8-X2L2-RMFG.

Garfunkel, Z., and Ben-Avraham, Z., 1996, The structure of the Dead Sea basin: Tectonophysics, v. 266, p. 155–176, doi: 10.1016/S0040-1951(96)00188-6.

Garfunkel, Z., and Derin, B., 1985. Permian-Early Mesozoic tectonism and continental margin formation in Israel and its implications for the history of the Eastern Mediterranean, *in* Dixon, J.E., and Robertson, A.H.F., eds., The geological evolution of the eastern Mediterranean: Oxford, Blackwell, Special Publication of the Geological Society No. 17, p. 187–201.

Green, P.F., Duddy, I.R., Gleadow, A.J.W., Tingate, P.R., and Laslett, G.M., 1986, Thermal annealing of fission tracks in apatite. 1: A qualitative description: Chemical Geology, v. 59, p. 237–253, doi: 10.1016/0009-2541(86)90048-3.

Greiling, R.O., Abdeen, M.M., Dardir, A.A., El Akhal, H., El Ramly, M.F., El Din Kamal, G.M., Osman, A.F., Rashwan, A.A., Rice, A.H.N. and Sadek, M.F., 1994, A structural synthesis of the Proterozoic Arabian-Nubian shield in Egypt: Geologische Rundschau, v. 83, no. 3, p. 484–501.

Gvirtzman, G., and Weissbrod, T., 1985, The Hercynian Geanticline of Helez and the Late Palaeozoic history of the Levant, *in* Dixon, J.E., and Robertson, A.H.F., eds., The geological evolution of the eastern Mediterranean: Oxford, Blackwell, Special Publication of the Geological Society No. 17.

Gvirtzman, Z., 2004, Chronostratigraphic table and subsidence curves of southern Israel: Israel Journal of Earth Sciences, v. 53, no. 1, p. 48–61, doi: 10.1560/KRH0-1Q21-U1YG-YH4H.

Hargrove, U.S., Stern, R.J., Kimura, J.-I., Manton, W.I., and Johnson, P.R., 2006, How juvenile is the Arabian-

Nubian Shield?: Evidence from Nd isotopes and pre-Neoproterozoic inherited zircon in the Bi'r Umq suture zone, Saudi Arabia: Earth and Planetary Science Letters, v. 252, p. 308–326, doi: 10.1016/j.epsl.2006.10.002.

Harlavan, Y., 1992, Geochronology of clay minerals in the Paleozoic section of southern Israel: Geological Survey of Israel report 2-92, 150 p. (in Hebrew).

Hauzenberger, C.A., Sommer, H., Fritz, H., Bauernhofer, A., Kröner, A., Hoinkes, G., Wallbrecher, E., and Thöni, M., 2007, SHRIMP U-Pb zircon and Sm-Nd garnet ages from the granulite-facies basement of SE Kenya: Evidence for Neoproterozoic polycyclic assembly of the Mozambique Belt: The Geological Society of London, v. 160, p. 745–757.

Heimann, A., Eyal, Y., Eyal, M., and Foland, K.F., 1995, Thermal events and low temperature alteration in the Precambrian schistose dykes and their host rocks in the Eilat area, southern Israel: $^{40}Ar/^{39}Ar$ geochronology, *in* Baer, G., and Heimann, A., eds., Physics and chemistry of dykes: Rotterdam, Balkema, p. 281–292.

Hurford, A.J., and Green, P.F., 1983, The zeta age calibration of fission track dating: Isotope Geoscience, v. 1, p. 285–317.

Ibrahim, K.M., and McCourt, W.J., 1995, Neoproterozoic granitic magmatism and tectonic evolution of the northern Arabian Shield: Evidence from southwest Jordan: Journal of African Earth Sciences, v. 20, no. 2, p. 103–118, doi: 10.1016/0899-5362(95)00037-T.

Jacobs, J., and Thomas, R.J., 2004, Himalayan-type indenter-escape tectonics model for the southern part of the late Neoproterozoic-early Paleozoic East African-Antarctic orogen: Geology, v. 32, p. 721–724, doi: 10.1130/G20516.1.

Jarrar, G., Wachendorf, H., and Zellmer, H., 1991, The Saramuj conglomerate: Evolution of a Pan-African molasse sequence from south-west Jordan: Neues Jahrbuch für Geologie und Paläontologie, Monatshefte, v. 6, p. 335–356.

Jarrar, G., Wachendorf, H., and Zachmann, D., 1993, A Pan-African alkaline pluton intruding the Saramuj conglomerate, south-west Jordan: International Journal of Earth Sciences, v. 82, no. 1, p. 121–135, doi: 10.1007/BF00563275.

Johnson, P.R., and Woldehaimanot, B., 2003, Development of the Arabian-Nubian Shield: Perspectives on accretion and deformation in the northern East African Orogen and assembly of Gondwana, *in* Yoshida, M., Windley, B.F., and Dasgupta, S., eds., Proterozoic East Gondwana: Supercontinent assembly and breakup: The Geological Society of London Special Publication 206, p. 289–325.

Jonckheere, R., Ratschbacher, L., and Wagner, G.A., 2003, A repositioning technique for counting induced fission tracks in muscovite external detectors in a single-grain dating of minerals with low and inhomogeneous uranium concentrations: Radiation Measurements, v. 37, p. 217–219, doi: 10.1016/S1350-4487(03)00029-5.

Jonckheere, R., Enkelmann, E., Min, M., Trautmann, C., and Ratschbacher, L., 2007, Confined fission tracks in ion-irradiated and step-etched prismatic sections of Durango apatite: Chemical Geology, v. 242, p. 202–217, doi: 10.1016/j.chemgeo.2007.03.015.

Katz, O., Beyth, M., Miller, N., Stern, R., Avigad, D., Basu, A., and Anbar, A., 2004, A Late Neoproterozoic (~630Ma) Boninitic Suite from southern Israel: Implications for the Consolidation of Gondwanaland: Earth and Planetary Science Letters, v. 218, p. 475–490, doi: 10.1016/S0012-821X(03)00635-6.

Kennedy, W.Q., 1964, The structural differentiation of Africa in the Pan-African tectonic episode: Leeds University Institute of African Geology 8th Annual Report, p. 48–49.

Ketcham, R.A., 2005, Forward and inverse modeling of low-temperature thermochronometry data: Reviews in Mineralogy and Geochemistry, v. 58, p. 275–314, doi: 10.2138/rmg.2005.58.11.

Kohn, B.P., Feinstein, S., and Eyal, M., 1990, Cretaceous to present paleothermal gradients, central Negev, Israel: Constraints from fission track dating: Nuclear Tracks and Radiation Measurements, v. 17, p. 381–388, doi: 10.1016/1359-0189(90)90061-2.

Kohn, B.P., Eyal, M., and Feinstein, S., 1992, A major Late Devonian–Early Carboniferous (Hercynian) thermotectonic event at the NW margin of the Arabian-Nubian shield: Evidence from zircon fission track dating: Tectonics, v. 11, no. 5, p. 1018–1027, doi: 10.1029/92TC00636.

Kolodner, K., Avigad, D., McWilliams, M., Wooden, J.L., Weissbrod, T., and Feinstein, S., 2006, Provenance of north Gondwana Cambrian-Ordovician sandstone: U-Pb SHRIMP dating of detrital zircons from Israel and Jordan: Geological Magazine, doi: 10.1017/S0016756805001640.

Küster, D., and Harms, U., 1998, Post-collisional potassic granitoids from the southern and northwestern parts of the Late Neoproterozoic East African Orogen: A review: Lithos, v. 45, p. 177–195, doi: 10.1016/S0024-4937(98)00031-0.

Landing, E., Bowring, S.A., Davidek, K.L., Westrop, S.R., Geyer, G., and Heldmaier, W., 1998, Duration of the Early Cambrian: U-Pb ages of volcanic ashes from Avalon and Gondwana: Canadian Journal of Earth Sciences, v. 35, p. 329–338, doi: 10.1139/cjes-35-4-329.

Lovera, O.M., Richter, F.M., and Harrison, T.M., 1989, The $^{40}Ar/^{39}Ar$ thermochronometry for slowly cooled samples having a distribution of diffusion domain sizes: Journal of Geophysical Research, v. 94, no. B12, p. 17,917–17,935, doi: 10.1029/JB094iB12p17917.

Lovera, O.M., Heizler, M.T., and Harrison, T.M., 1993, Argon diffusion domains in K-feldspar II: Kinetic properties of MH-10: Contributions to Mineralogy and Petrology, v. 113, p. 381–393, doi: 10.1007/BF00286929.

Lovera, O.M., Grove, M., Kimbrough, D.L., and Abbott, P.L., 1999, A method for evaluating basement exhumation histories from closure age distributions of detrital minerals: Journal of Geophysical Research, v. 104, no. B12, p. 29,419–29,438, doi: 10.1029/1999JB900082.

McGill, R., Tukey, J.W., and Larsen, W.A., 1978, Variations of box plots: The American Statistician, v. 32, p. 12–16, doi: 10.2307/2683468.

Meert, J.G., 2003, A synopsis of events related to the assembly of eastern Gondwana: Tectonophysics, v. 362, no. 1, p. 1–40, doi: 10.1016/S0040-1951(02)00629-7.

Meesters, A.G.C.A., and Dunai, T.J., 2002, Solving the production-diffusion equation for finite diffusion domains of various shapes Part II. Application to cases with alpha-ejection and nonhomogeneous distribution of the source: Chemical Geology, v. 186, p. 347–363, doi: 10.1016/S0009-2541(02)00073-6.

Parnes, A., 1971, Late Lower Cambrian trilobites from the Timna area and Har Amram (southern Negev, Israel): Israel Journal of Earth Sciences, v. 20, p. 179–205.

Powers, R.W., Ramirez, L.F., Redmon, C.D., and Elberg, E.L., Jr., 1966, Geology of the Arabian Peninsula: Sedimentary geology of Saudi Arabia: U.S. Geological Survey Professional Paper 560-D, 127 p.

Quennell, A.M., 1958, The structural and geomorphic evolution of the Dead Sea rift: Quarterly Journal of the Geological Society of London, v. 114, p. 2–24.

Rahn, M.K., Brandon, M.T., Batt, G.E., and Garver, J.I., 2004, A zero-damage model for fission-track annealing in zircon: The American Mineralogist, v. 89, p. 473–484.

Renne, P.R., Swisher, C.C., Deino, A.L., Karner, D.B., Owens, T., and Depaolo, D.J., 1998, Intercalibration of standards, absolute ages and uncertainties in $^{40}Ar/^{39}Ar$ dating: Chemical Geology, v. 145, p. 117–152, doi: 10.1016/S0009-2541(97)00159-9.

Rossetti, F., Cozzupoli, D., and Phillips, D., 2008, Compressional reworking of the East African Orogen in the Uluguru Mountains of eastern Tanzania at c. 550 Ma: Implications for the final assembly of Gondwana: Terra Nova, v. 20, no. 1, p. 59–67.

Saxena, S.K., 1966, Evolution of zircons in sedimentary and metamorphic rocks: Sedimentology, v. 6, p. 1–33, doi: 10.1111/j.1365-3091.1966.tb01568.x.

Segev, A., 1984, Lithostratigraphy and paleogeography of the marine Cambrian sequence in southern Israel and southern Jordan: Israel Journal of Earth Sciences, v. 33, p. 26–33.

Segev, A., 1992, Remobilization of uranium and associated metals through karstification processes: A case study from the Timna Formation (Cambrian), southern Israel: Ore Geology Reviews, v. 7, p. 135–148, doi: 10.1016/0169-1368(92)90009-A.

Segev, A., Halicz, L., Steinitz, G., and Lang, B., 1995, Post-depositional processes on a buried Cambrian sequence in southern Israel, north Arabian Massif: Evidence from new K-Ar dating of Mn-nodules: Geological Magazine, v. 132, no. 4, p. 375–385.

Shackleton, N., 1996, The final collision zone between East and West Gondwana: Where is it?: Journal of African Earth Sciences, v. 23, no. 3, p. 271–287.

Sneh, A., Bartov, Y., Weissbrod, T., and Rosensaft, M., 1998, Geological map of Israel: Israel Geological Survey, 1:200,000, 4 sheets.

Stern, R.J., 1994, Arc-assembly and continental collision in the Neoproterozoic East African Orogen: Implications for the consolidation of Gondwanaland: Annual Review of Earth and Planetary Sciences, v. 22, p. 319–351.

Stern, R.J., and Hedge, C.E., 1985, Geochronologic and isotopic constraints on Late Precambrian crustal evolution in the Eastern desert of Egypt: American Journal of Earth Science, v. 285, p. 97–127.

Summer, N.S., Kohn, B.P., Ito, H., Ayalon, A., and Kolodny, Y., 1995, Isotopic and chronological constraints on dyke emplacement, Makhtesh Ramon, southern Israel, *in* Baer, G., and Heimann, A., eds., Physics and chemistry of dykes: Rotterdam, Balkema.

Unrug, R., 1997, Rodinia to Gondwana: The geodynamic map of Gondwana supercontinent assembly: GSA Today, v. 7, no. 1, p. 1–6.

Vermeesch, P., 2004, How many grains are needed for a provenance study?: Earth and Planetary Science Letters, v. 224, no. 3–4, p. 441–451, doi: 10.1016/j.epsl.2004.05.037.

Villa, I.M., 2006, From nanometer to megameter: Isotopes, atomic-scale processes, and continent-scale tectonic models: Lithos, v. 87, p. 155–173, doi: 10.1016/j.lithos.2005.06.012.

Weissbrod, T., 1980, The Paleozoic of Israel and adjacent countries [Ph.D. thesis]: Jerusalem, Hebrew University, 275 p. (in Hebrew).

Weissbrod, T., and Nachmias, J., 1986, Stratigraphic significance of heavy minerals in the late Precambrian-Mesozoic clastic sequence ("Nubian Sandstone") in the Near East: Sedimentary Geology, v. 47, p. 263–291, doi: 10.1016/0037-0738(86)90086-2.

Weissbrod, T., and Sneh, A., 2002, Sedimentology and paleogeography of the late Precambrian-early Cambrian arkosic and conglomeratic facies in the northern margins of the Arabo-Nubian Shield: Geological Survey of Israel Bulletin No. 87, 44 p.

Willis, K.M., Stern, R.J., and Clauer, N., 1988, Age and geochemistry of Late Precambrian sediments of the Hammamat series from Northeastern Desert of Egypt: Precambrian Research, v. 42, p. 173–187, doi: 10.1016/0301-9268(88)90016-2.

Manuscript Received 30 May 2008
Revised Manuscript Received 1 October 2008
Manuscript Accepted 6 October 2008

Printed in the USA